Design, Modeling and Simulations of a Cabinet Safe System for a Linear Particle Accelerator of Intermediate-Low Energy by Optimization of the Beam Optics

C. O. Maidana [1,2], A. W. Hunt [2]

[1] Idaho Accelerator Center – 1500 Alvin Ricken Drive, Pocatello, Idaho, 83201, USA
[2] Idaho National Laboratory, PO Box 1625, Idaho Falls, Idaho 83415-3855, USA

Email contact of main author: maidana@physics.isu.edu

As part of an accelerator based Cargo Inspection System, studies were made to develop a Cabinet Safe System by Optimization of the Beam Optics of Microwave Linear Accelerators of the IAC-Varian series working on the S-band and standing wave $\pi/2$ mode. Measurements, modeling and simulations of the main subsystems were done and a Multiple Solenoidal System was designed.

This Cabinet Safe System based on a Multiple Solenoidal System minimizes the radiation field generated by the low efficiency of the microwave accelerators by optimizing the RF waveguide system and by also trapping secondaries generated in the accelerator head. These secondaries are generated mainly due to instabilities in the exit window region and particles backscattered from the target. The electron gun was also studied and software for its right mechanical design and for its optimization was developed as well. Besides the standard design method, an optimization of the injection process is accomplished by slightly modifying the gun configuration and by placing a solenoid on the waist position while avoiding threading the cathode with the magnetic flux generated.

The Multiple Solenoidal System and the electron gun optimization are the backbone of a Cabinet Safe System that could be applied not only to the 25 MeV IAC-Varian microwave accelerators but, by extension, to machines of different manufacturers as well. Thus, they constitute the main topic of this paper.

1. Introduction

National and international security concerns have led to an increase in research efforts that focus on the detection and identification of potentially dangerous fissionable material. Such efforts have produced several detection techniques. Many of them use a mobile linear particle accelerator with energy in the range of 8 to 25 MeV for cargo inspection [1]. Many even lower energy accelerators systems (<1 MeV) have already established "cabinet safe" operation within several meters of the accelerator, largely due to an ease of shielding low energy photons, rather than novel engineering [2]. Higher energy systems (1 – 25 MeV), as the ones required for cargo inspection, need the same convenience and portability as low energy systems for their transportation and operation in harbors and borders. To accomplish the latter the shielding needs to be minimized, meaning a reduction of the radiation field must be done by other means such as beam optics optimization. Modeling, simulation and optimization of the IAC-Varian accelerators were done in first place [3] followed by radiation studies of the standard and optimized models of the accelerators.

2. Beam Dynamics Studies of the IAC Microwave Linacs

The modeling process of the IAC-Varian accelerator series' waveguide was divided in three main parts: RF cavities, confining solenoids and beam characteristics. Each part was then subdivided in smaller ones as explained in the previous work done by these authors [3].
The determination of the main accelerating field, which is the TM_{010} mode, was done analytically [4] and from this solution, a table was generated for its use within the code ASTRA [5], which calculates the transverse field components from the derivatives of the on axis field. The later code allows the inclusion of apertures and material properties for

secondary electron emission as well. As explained by Floetmann et al. [5, 6], when an electron hits an aperture ASTRA generates a random integer number of secondaries according to certain intrinsic model function using a Poisson generator. The secondary electrons are emitted isotropically and the emission position of the secondary electrons is corrected to surface boundaries.

The RF cavities that constitute the waveguide are surrounded by two long solenoids to confine the electrons to the waveguide and to minimize multipacting. A table of the axial magnetic field was generated from measurements using an axial magnetic probe for its computation within ASTRA.

The third point in consideration is the beam itself, a Plateau distribution for the macro-bunch and a Gaussian distribution for the micro-bunch. The efficiency was measured to be of ~10%; roughly 90% of the beam generated in the source is lost, nearly 66% in the injection process in the first half –bunching- cavity [7].

For the RF waveguide simulation, 8000 macro particles were taken into account in Gaussian distribution with a width $\sigma_{x,y}$ of 0.75 mm and a micro bunch charge of -2nC, being the initial energy of the particles injected in the guide of 50 KeV. The particles were distributed quasi-randomly following the Hammersley sequence, a quasi-Monte Carlo deterministic method. In this way, statistical fluctuations are reduced and artificial correlations are avoided. ASTRA was used for the beam dynamics studies due to its intrinsic algorithm for space charge tracking. ASTRA tracks particles based on a Runge-Kutta integration of 4th order with fixed time step through the user defined external fields taking into consideration the space charge field of the particle cloud [5]. A cylindrical grid, consisting of rings and slices, was set up over the bunch extension for the space charge calculations. The space charge effect is a principal cause of emittance growth when the beam energy is low.

In FIG. 1 the longitudinal particle position of the lost particles is shown. We see that the majority of the electrons are lost in the first group of cavities and only ~10.89% of the initial charge reach the exit of the waveguide, which is located at ~1.33 m. The secondary electrons that reach the end of the waveguide were estimated to be of 0.0025% of the injected charge, being the total secondary electrons produced inside the waveguide equivalent to 0.0213% of the injected one. The average energy contributed by the TM_{010} mode was estimated in ~14 MeV. These numbers are in very good agreement with the experimental results, as expected.

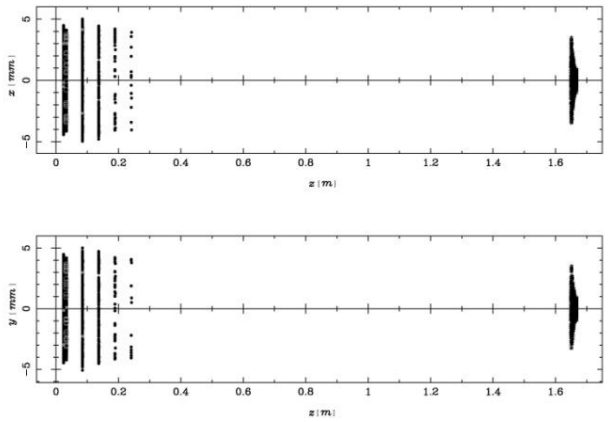

FIG. 1: Longitudinal particle position on IAC-Varian Accelerator Series showing the interaction point of the electrons with the waveguide and with the target. The stars represent the normal macro-particles reaching the target; the darker circles represent lost macro-particles and the gray ones are macro-particles traveling backwards. Secondaries generated at the exit window are not shown.

3. Radiation Studies for IAC Microwave LINACS

3.1. Gamma Showers Results using Monte-Carlo Methods

Using the Monte Carlo code PENELOPE 2006 to perform simulations of electron-photon transport, a basic accelerator head with a water phantom was studied. The electron beam was set to 18 MeV, the tungsten target to 2 mm thickness and the water phantom to 30 cm. The target was localized 10 cm from the LINAC exit port. The angular distribution of the backscattered electrons shows that the majority are backscattered in the 0 to 45 degrees region relative to the negative z-axis, as seen in FIG. 2. The energy distribution for the backscattered electrons shows that more than 90% of such electrons have an energy that is less than 3 MeV; with the majority between 0 and 1.5 MeV. As a result of this study, it was concluded that ~ 0.346% of the primary electrons are backscattered.

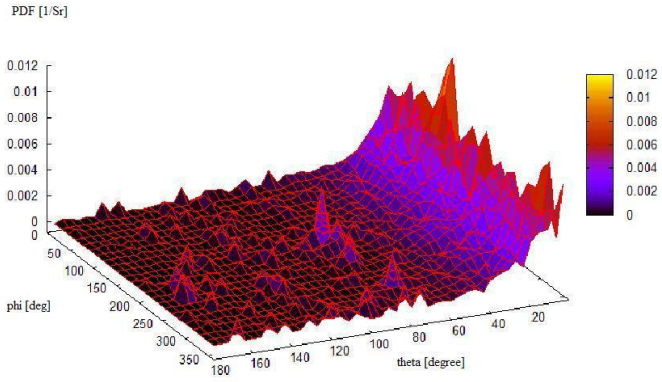

Fig. 2: Angular distribution of the backscattered electrons for an 18 MeV electron beam hitting a 2mm W target taking into account the production of γ showers. The main part of the electrons is backscattered in the range 0 to 45^{o} with some components at 70^{o}+ angles.

3.2. Production of X Rays by RF cavities

The X-rays produced in the RF cavities are mainly the result of bremsstrahlung from dark current, secondaries and off-orbit primaries hitting the body of the cavities. At the beginning of the RF waveguide, the X-ray production is relatively low in energy, with electron ranges (track lengths) not large enough to allow an electromagnetic shower development but large enough to produce bremsstrahlung at significant depths in a Cu structure, as explained by J. Norem et al. in [8]. Unfortunately, the radiation around RF cavities is not entirely predictable (even carrying erratic components) depending on the surface conditions which change with time.

Using the Los Alamos National Laboratory code MCNPX, a basic waveguide structure of the pillbox type for the cavities running at their respective average accelerating energy for a final beam of 18 MeV was modeled; then emission of radiation from the cavities under study was simulated. For the beam structure a macro bunch of time length T_p = 1 μs, repetition frequency f_{rep} = 120 Hz, klystron RF frequency f_{RF} = 2.856 GHz and 3000 micro-bunches were used. Each energy was run with a total of $40 \cdot 10^6$ (forty million) electrons in each appropriate accelerator cavity. The photon spectra going through an empty phantom 1 m from the accelerator 90 deg with 720 μA injected current can be seen in FIG. 3. Using the 1977 ANSI/ANS flux-to-dose conversion factors and making use of the calculated photon yield information, one can obtain a dose rate produced by the first group of cavities (main responsible for the waveguide lateral dose), as shown in Fig. 4. These values are an

approximation to the real dose rate emitted due to the fact that the flux-to-dose conversion factors have an uncertainty of around 20%. Other sources of uncertainties are the shape of the macro-bunch (which cannot always be described as plateau or Gaussian), shape of the cavity, the exact length of the pulse, the acceptance of the electrons in the RF cavities (all "RF buckets" filled) and electron gun efficiency in the repetition frequency. The dose rate represented in FIG. 4 is for an electron beam with a final energy 18 MeV and an injected charge q = 2 nC/micro-bunch in the micro-structure and 68.4 μA average output current. The total dose rates calculated are ~ 95 R/h for a water phantom (side distance = 1 m) and ~ 116 R/h for the empty phantom (side distance = 1 m). The water phantom is used to simulate the absorption and scattering properties of soft tissue and muscle; and so, to calculate the deposited dose that a human being would suffer due to the fact that more than 70% of our body contains water. The dose rate calculations in both phantoms were done in a different way to get independent results to compare. For the empty phantom, the photon flux was first obtained and then the dose factors provided by ANSI/ANS were applied. For the water phantom, the energy deposited was first calculated and from there the deposited dose was obtained.

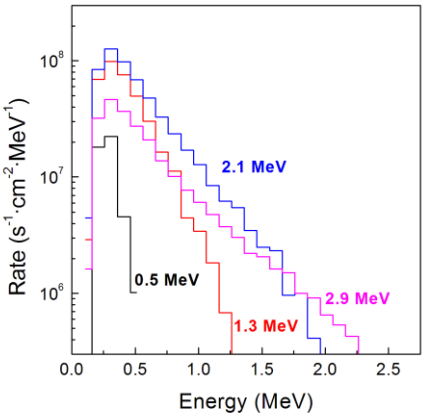

FIG. 3: Photon flux spectra going through an empty phantom 1 m from the accelerator 90 deg with 720 μA injected. The spectrum was generated by MCNPX using input data obtained from ASTRA and PENELOPE 2006. The normalization of the dose rate with respect to the energy was done to ease the integration.

Comparing these results with the ones obtained experimentally in [2] and the results published by NCRP Report 144, a good qualitative agreement between simulation and experiments can be found, which support the procedure followed in the modeling and simulation process. For the case of NCRP Report 144, the dose rate absorbed by a medium Z, thick target, and produced by a 18 MeV electron beam was established to be between 150 and 200 R/h at 1 m, sideward direction, from the target. Our calculations show a value of ~115 R/h, which is in good agreement with NCRP. In the case of the measurements reported in [2] using a small medical T4 LINAC with an energy of 4 MeV and output current of 7.1 μA, a lateral dose rate between 3 and 16 R/h was measured at angles from 45 to 90 degrees relative to the accelerator axis. For a 7.1 μA output current the calculated dose rate from the IAC-Varian waveguide is 12 R/h, which is qualitatively consistent with [2]. One also has to consider that the accelerators are completely different and a more accurate study of that type of accelerator is not part of the scope of this research.

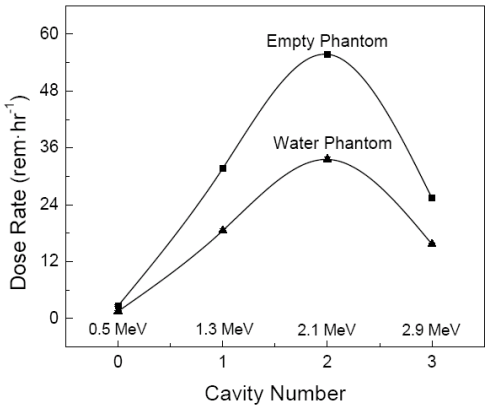

FIG. 4: Dose rate for the radiation emitted from the RF cavities ($T_b=1\mu s$, $f_{RF}=2.856GHz$, $f_{rep}=120Hz$, $I_{inj}=720\mu A$, $I_{out}=68.4\mu A$) calculated using the MCNPX conversion factors provided by Los Alamos National Laboratory.

4. Optimization System Development for IAC Microwave LINACS

As it is well known, a beam passing thru an RF cavity experiences not only acceleration and longitudinal bunching but also a transverse defocusing. By placing magnetic solenoids in the RF lattice, a transverse focusing can be achieved to counteract this effect. These fringe fields generated by coils extend over long distances and may contain several nonlinearities [9].

4.1. The Front-End Solenoid Approach

An approach to consider and study was the use of high field solenoids at the exit of the beam line. The idea behind the Front-End (F.E.) solenoids is to trap and/or confine the secondary particles generated at the exit port reducing in this way the radiation field.
The microwave LINACS of the IAC-Varian Series contains two relatively long solenoids around the waveguide. The goal of these solenoids is to confine the particles and keep them far from the waveguide's walls. The long confinement solenoid interacting with the F.E. solenoids has a measured half aperture of 0.127 m and a length of 1.04 m. Because the solenoid's fringe fields expand far in space, we have to take into account its influence in the F.E. solenoids' generated fields.
Using COSY Infinity's [10] Differential Algebra based numerical integrator (8^{th} order Runge Kutta w/automatic step size control), the transfer map for the F.E. solenoids was obtained as well as a file containing the value for the on-axis magnetic field for its inclusion in ASTRA. The value of the B field and the physical dimensions for the F.E. solenoids, corrected for the confinement solenoid's effect and calculated for an 18 MeV beam, can be found in TABLE 1.

TABLE I. Magnetic field and dimensions [m] for the F.E. solenoids based on 18 MeV electrons.

B_z [T]	Length	Aperture	Drift length
0.74509	0.13702	0.10153	0.11471

4.2. Development of a Multiple Solenoidal System

Based on the models developed by the authors of this paper a Multiple Solenoidal System was designed, as seen in FIG. 5, with the following characteristics:
-F.E. solenoids

- B_z field at the center of each solenoid, 0.745 T (fields of opposite signs)

• Drift lengths between: solenoids, 0.1147 m; first solenoid and LINAC, 0.05 m
• Aperture (radius), 0.1015 m; Length, 0.1370 m

-Thin solenoids

• B_z field at the center of each solenoid, 0.08718 T
• Aperture (radius), 0.14 m; Length, 0.025 m
• Located at 0.0005 m (0), 0.071 m (1), 0.228 m (4), 0.65 m (12) (cavity)

The computation was made by dividing the beam line in 1000 segments for the calculation of the statistical bunch parameters. The bunch length was divided in a grid of 25 longitudinal slices and 25 radial rings with automatic scaling for the space charge field calculation. The field at any point between the grid center points was calculated by means of a cubic spline interpolation to avoid possible numerical instabilities generated by the used of polynomials.

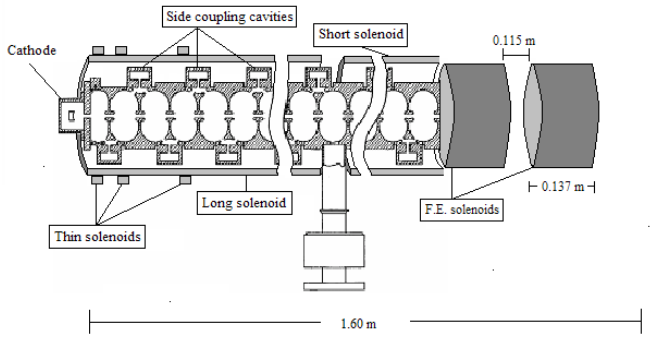

FIG. 5: Cross section diagram of the IAC-Varian microwave LINAC with the Multiple Solenoidal System.

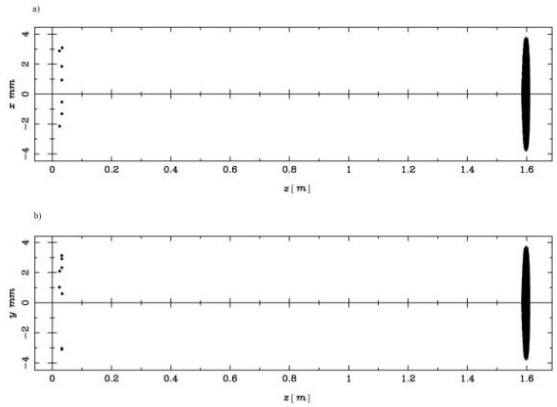

FIG. 6: Longitudinal particle interaction points for the Multiple Solenoidal System on IAC-Varian Accelerator waveguide at 18 MeV. More than 89% (±10%) of the injected particles reach the target. The secondaries generated and the particles lost on the exit port are not considered here.

The longitudinal particle positions over the waveguide, through the FE solenoids and up to a distance of 1.6 m from the injection point, are represented in FIG. 6. From the 8000 macro-particles injected, 7992 macro-particles reached the final position, which constitute a micro-bunch charge of ~1.99 nC (99% of the original charge). The number of active secondary electrons was greatly reduced as well as the energy spread. The estimated beam size is $\sigma_{x,y}$ ~1.9 mm. The divergence of the beam within the waveguide is well controlled after the initial critical points (injection into the half bunching cavity) due to the application of the magnetic fields that minimize the original divergence of 5+ mrads at the exit of the gun.

Combining these results with the Monte Carlo simulations done in section 3, the dose rate from the cavities where particles are lost can be calculated. The radiation emitted from the

buncher and first full cavitiy in the waveguide are the only important ones (less than 0.1 % of the injected charge is lost). The radiation dose-rate emitted by these cavities is calculated to be 5 mrads/h at 1 m from the accelerator and it could be as low as 1 mrad/h using the same dose-rate conversion factors used in section 3, depending of the final beam energy and other factors not discussed here. This is a 4 orders of magnitude decrease in lateral dose rate compared to the original IAC-Varian waveguide. Furthermore, a dose rate of 5 mR/hr is acceptable for a cabinet safe system and this has been accomplished without the addition of shielding material around the waveguide. The addition of shielding will decrease the dose rate even further. As it can be seen at first sight, huge improvements can be accomplished by the use of a Multiple Solenoidal System which encourage for further research to be done. The uncertainties in this work that one has to consider and minimize in further studies are given mainly by: • Maximum acceptance for a bunching system is ~80% (only accomplished in RFQ systems); • Wakefields modify the way that a cavity interacts with the beam and its calculations are still a topic of research; • Dipole mode, transverse fields deflecting the particles, could have some influence but limited by the beam loading (TM_{110} mode); • More accurate modeling of the RF cavities, including the bunching system, has to be done.

5. Electron Gun Characterization and Optimization

One of the most used electron guns in microwave particle accelerators is the Pierce Gun. Based on the Rodney-Vaughan method, software for the complete characterization and mechanical design of the gun was developed. A further study of the produced beam shows a non-uniform density profile distribution, FIG. 7, far from the Gaussian shape due to the strong space charge effects making its analysis more complex. A way to optimize the injection process is by placing a thin solenoid in the waist position avoiding threading the cathode. Time resolve images of such a system can be seen in Fig. 8.

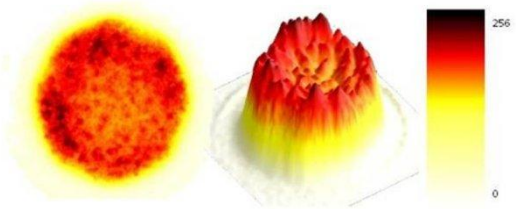

FIG. 7: Beam profile for electrons created in a Pierce gun (I=25mA, V=10keV). Notice the presence of strong space charge forces in its center. Picture by M. Hodek with measurements done with C. O. Maidana & A. Lichtl.

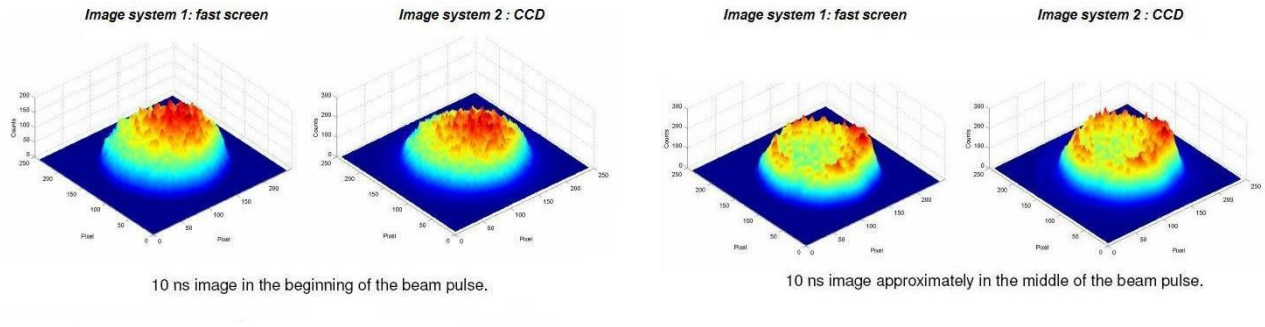

FIG. 8: Time resolved images of a low current electron beam generated in a Pierce gun after transport through a thin focusing solenoid. A higher density of electrons is appreciated in the front center of the beam while a higher electron density distribution is located at the edges in the middle of the beam pulse. Images taken by T. Da Silva.

6. Conclusions

Our calculations indicate that the Multiple Solenoidal System turns out to be a very good way to improve the efficiency of the accelerator waveguide and minimize the radiation generated. This implies a reduction in the shielding requirements. The lateral radiation dose emitted by the RF waveguide would be reduced up to 3 or even 4 orders of magnitude. At the same time, by capturing secondaries generated in the exit window section using F.E. solenoids, and by optimizing the beam dynamics, further reduction of the total dose could be achieved. The latter, together with the fact that the difficulties associated to the construction of a well shielded target can be over passed, and that the injection process can also be improved by optimizing the electron gun, constitute the basis for a Cabinet Safe System for microwave linear particle accelerators operating in the 8 to 25 MeV range. Future experimental work to benchmark these calculations, as feedback for the development of more advanced models and to verify these predictions are the natural steps to follow. We will then have a robust system for beam optimization and dose reduction from medical-industrial waveguides and related homeland security accelerators.

6. Acknowledgements

This research was developed thanks to the U.S. Department of Defense.

5. References

[1] M.T. KINLAW and A.W. HUNT – "Fissionable Isotope Identification Using the Time Dependence of Delayed Neutron Emission", Nuclear Instrumentation and Methods A, Elsevier, Proceedings of the 5th International Topical Meeting on Nuclear Research Applications and Utilization of Accelerators, Italy (2005).

[2] WELLS, JONES, YOON, HARMON – "Cabinet-safe study of 1-8 MeV electron accelerators", Nuclear Instrumentation and Methods in Physics Research A463 (2001).

[3] C.O. MAIDANA and A.W. HUNT – "Modeling, Simulation and Optimization of Microwave LINACS of the 25 MeV IAC series", 6th International Topical Meeting on Nuclear Research Applications and Utilization of Accelerators, USA (2007).

[4] C.O. MAIDANA, "Design, modeling and simulations of a cabinet safe system for a linear particle accelerator of intermediate-low energy by optimization of the beam optics, Idaho State University", Ph.D. thesis (2007).

[5] K. FLOETMANN, ASTRA, A space charge tracking algorithm, http://www.desy.de/~mpyflo/Astra_dokumentation/.

[6] M.A. FURMANN, M.T. PIVI, "Probabilistic model for the simulation of secondary electron emission", PRST-AB 5, 124404 (2002).

[7] C.J. KARZMARK, C.S. NUNAN and E. TANABE, Medical Electron Accelerators, McGraw Hill Inc, USA.

[8] J. NOREM, A. MORETTI and M. POPOVIC, "The radiation environment in and near gradient rf cavities", Nuclear Instruments and Methods in Physics Research A472 (2001).

[9] C.O. MAIDANA, K. MAKINO and M. BERZ, "Muon beam ring cooler simulations using COSY INFINITY", Institute of Physics Conference Series N175, 7th International Computational Accelerator Physics Conference, USA (2004).

[10] M. BERZ and K. MAKINO, COSY INFINITY Version 8.1 – User's guide and Reference manual. Technical Report MSUHEP-20704, Department of Physics and Astronomy, Michigan State University, East Lansing, MI 48824 (2001). See also http://cosy.pa.msu.edu.